Li-ion Batteries for Providing Virtual Inertia

Lennart Beushausen
Technical University of Clausthal
Institute of Electrical Power Engineering and Energy Systems
Clausthal-Zellerfeld, Germany
Lennart.beushausen@tu-clausthal.de

J. Gollenstede, F. Deblon, R. Benger,
H.-P. Beck
Clausthal University of Technology

Lithium-ion batteries are essential for the contemporary society. The significance and demand for batteries are constantly increasing. The change in li-ion batteries is not only important in terms of electro mobility but also in stationary storage systems. Recent developments lead towards decentralized energy resources powering electric systems. Those systems require adapted and optimized power and energy storage systems. This paper will indicate the special constrains and requirements for batteries providing ancillary services – in particular virtual inertia – and points out preliminary results of battery behavior for example aging, used for grid stabilization.

I. INTRODUCTION

Providing power and inertia is necessary to secure a stable energy supply, which requires an equilibrium of supplied and consumed power at any time (compare fig. 1). Inertia is especially used for damping fast frequency changes. Beside the commercial possibilities of providing inertia for grid stabilization, it is also possible to use fast responding power elecronics, so-called virtual generated inertia.

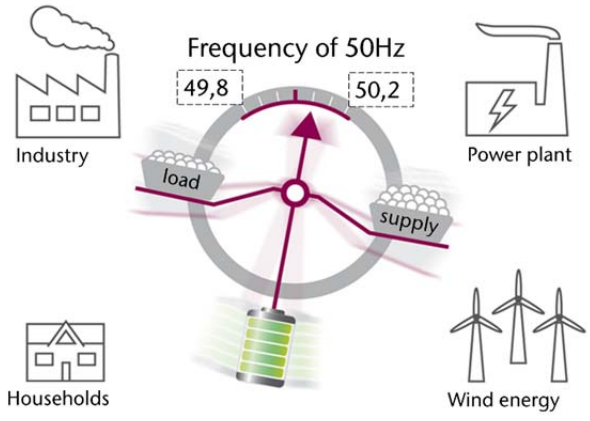

Figure 1: Principle of providing an equilibrium of supplied and consumed power in the electrical grid

The objectives of the public research project "Momentanreserve mit Hochleistungs-batterien (ReserveBatt)" (Virtual inertia by high power batteries) funded by the Federal Ministry for Economic Affairs and Energy are to build and evaluate a 400 kVA battery-inverter demonstrator to provide instantaneous virtual inertia from high power li-ion batteries.

This concept requires the implementation of the VSG algorithm "Virtual Synchronous Machine (VISMA)". The battery replaces the physical inertia of a synchronous generator in a conventional power plant which stored comparatively high energy in the transmission. Furthermore the design and evaluation of utilization options and possible business models for the provision of ancillary services are of importance.

This paper presents primarily results gathered in the project. On the one hand, ancillary services are presented. On the other hand a possibility to provide inertia is specified. Furthermore, there is a focus on the battery behavior, in detail the battery aging, when providing virtual inertia and other ancillary services by high power density li-ion batteries. The battery performance and aging under high dynamic loads is analyzed and examined with laboratory cells, consumer cells and modules.

II. GENERAL OVEWVIEW OF ANCILLARY SERVICES

Ancillary services generate an equilibrium of load and supply by provoding control reserve power (compare fig. 2). In physical behavior there are two different ancillary services:

a) The propotional power to frequency deviation:
This power is seperated into primary (black), secondary (grey), tertiary or minute (white) control power and hour reserve (violet).

b) The proportional power to frequency gradient:
This classification is the inherent, stabilizing characteristic of the rotating mass of generators. They provide inertia

power reserve damping the initial frequency change caused by an imbalance.

The general ability of a power plant to supply inertia is described by the inertia constant H, which is the quotient of kinetic energy of the generator turbine system E and the rated apparent power S.

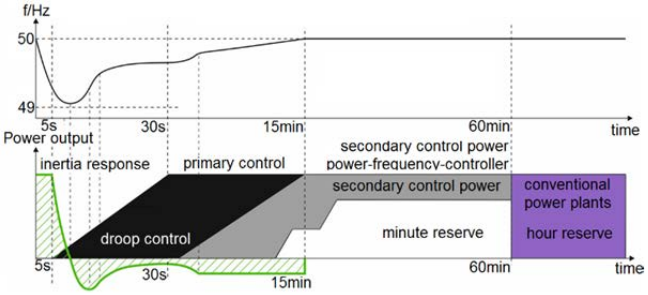

Figure 2: Inertia power response (green) during a frequency drop incident with an exemplary frequenzy nadir close to 49Hz in comparison with control reserve power [1].

Figure 2 shows the frequency stabilization mechanisms after five seconds such as primary and secondary control power are activated and the frequency restores to 50Hz. The instantanious reaction of the inertia keeps the frequency deviation limited until other control mechanism can take apart.

III. THE VIRTUAL SYNCHRONOUS MACHINE

The developed hardware system of the project mainly consists of a high performance lithium-ion battery system and a power converter (S=400kVA). The converter consists of intelligent power modules (IPM) and connects the battery system to the distribution network (compare figure 3).

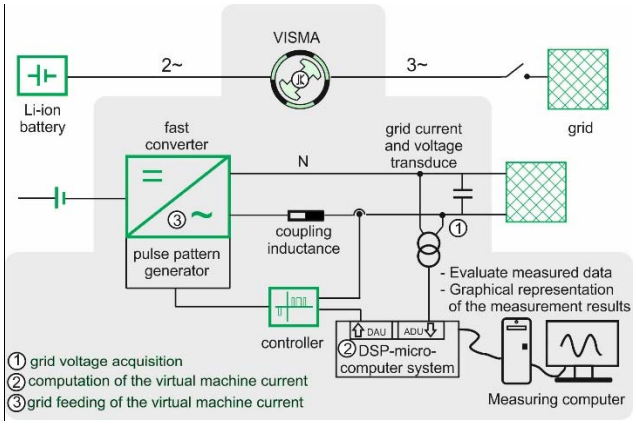

Figure 3: Fundamental set-up of the virtual synchronous machine with measurement of grid current and voltage (1), computation of the virtual machine current on a digital signal processor (DSP) (2) and the inverter as power module grid connection (3) provided by a DC-link (energy storage) [2].

A digital signal processor (DSP) controlls the converter. The DSP uses the optimized virtual synchronous generator (VSG) algorithm of the TU Clausthal, the virtual synchronous machine (VISMA) [14] to calculate the virtual machine current as control variable.

Basic equation for the VSG algorithm is the general torque equation [2]:

$$M_{mech} - M_{el} - M_d = J \cdot \frac{d\omega_r}{dt} \quad (1)$$

M_{mech} is the mechanical, M_{el} the electrical and M_d the damping torque. Because the system is running without a steam turbine in a virtual machine, the set value of M_{mech} can be parameterized directly in terms of the desired working point. M_{el} can be calculated directly over the injected power P_e and the machine's rotor angle velocity ω_r:

$$M_{el} = \frac{P_e}{\omega_r} \quad (2)$$

The damping torque represents the internal swinging of the rotor and is caused by leaving a stationary operating point, which depends on the filter time constant T_d and the damping factor k_d:

$$M_d = k_d \cdot \frac{d\omega_r}{dt} - T_d \frac{dM_d}{dt} \quad (3)$$

The equivalent circuit of a synchronous three-phase virtual stator is generated by the voltage e_i, the stator inductance L_i, the real part of the windings R_i and counter-voltage from the grid u_i:

$$e_i = i_i R_i + L_i \frac{di_i}{dt} + u_i \quad (4)$$

The VSG-algorithm calculates the required current values instantaneously. These reference values are transferred to the control unit of the power converter system.

IV. LOAD PROFILE STOCHASTICS FOR THE VIRTUAL SYNCHRONOUS GENERATOR

With the rated power of P=400kW, the converter system has to react on different frequency profiles. These profiles result directly from the frequency gradient and the inertia constant J (cmpr. (1)). To optimize the operating grade, the frequency must be studied.

Hence, high-resolution measurements are performed for grid frequency rate of change of frequency (ROCOF). That procedure allows an estimation of load profiles, in terms of stochastics.

With aquisition to (1), a high inertia constant J leads to a limitation of small ROCOFs. Vice versa, the operating grade will be low. Three examples of the covered certainties (3σ to 1.96σ of observed ROCOFs) are presented in fig. 4. This allows the approach with different gaussian distributions to estimate affilated battery load profiles in this operation mode.
Simulations and battery aging tests are developed out of those load distributions[1].

[1] Detailed analyses will be presented at the EPE conference 2018

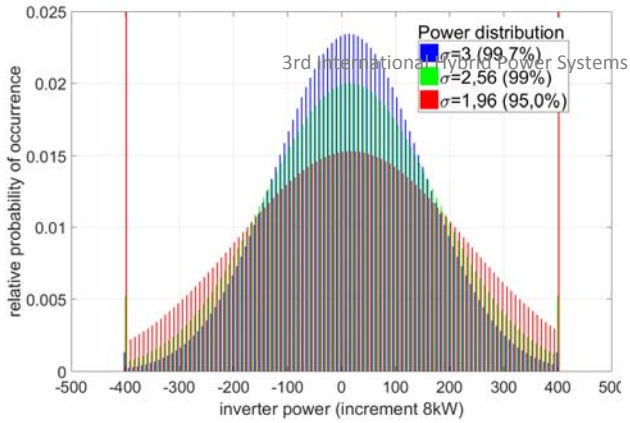

Figure 4: Possible loads on a battery system when providing virtual inertia with the VISMA and a 400kVA converter system (based on intern data of the Tennet GmbH).

Adapted to primary control power, so to charge and discharge out of the initial state equally, the SOC of 50% is set and will be used for further analyses of the battery.

V. LITHIUM ION BATTERIES

If stationary batteries are predestinated for the provision of ancillary services in the grid, it can be assumed that they need to cover only a small change in SOC and remain at an intermediate SOC range in order to provide both, negative and positive control power. Especially the cycling around 50% SOC is decisive. The DOD cycle depth is primarily around 5-10%. First research results of cycled LFP/graphite batteries are shown in figure 5. It shows a significantly higher aging process for LFP batteries at 55% SOC and a 10% DOD [10]. The other load profiles have less impact on the aging process.

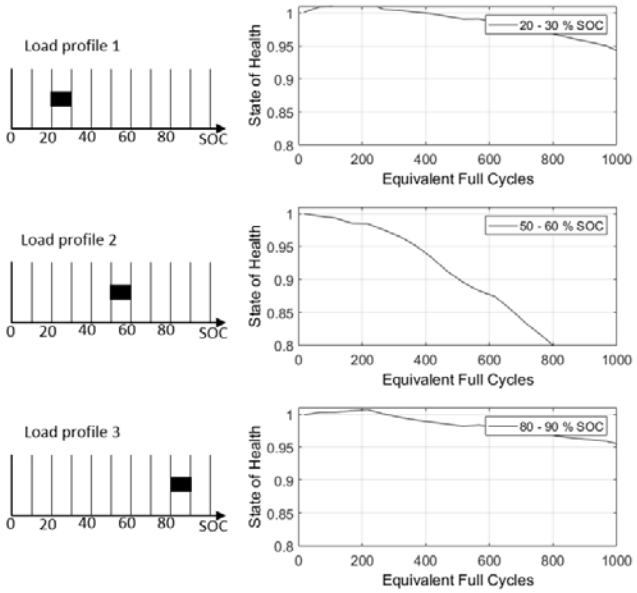

Figure 5: Comparison of the differential aging processes over equivalent full cycles from LFP cells by 40°C and a current rate of 2C.

A general aproach to explain this behavior are the steps of the electrochemical intercalation process of lithium-ions into the graphite layer [9]. A simplified demonstation of the process is presented in figure 6.

By periodically passing through the different stages of intercalation an increased aging is expected. One of these transitions of the intercalation stages is in the range of 55% SOC. An increase in volume change during the intercalation process could be responsible for the accelerated aging effect [12] [13].
At the beginning of the charging process all stages of the anode materials are unoccupied. During this charging process the electrostatic repulsion of the embedded lithium ions are the cause to occupy preferable remote and not the adjacent layers [8]. Accordingly, at the end of the charging process, all layers are occupied, which corresponds to the lithium concentration of the anode of LiC_6 (stage 1). A completely discharged battery in stage 4 contains LiC_{30}.

Further analyses of the influence from SOC range on aging with a current rate corresponding to 1C and a change in DOD (ΔDOD) of 30 % were performed on NMC/graphite batteries.
Various cell sizes like laboratory cells, small commercial round cells and high power pouch cells up to 70Ah have been studied.

Figure 7 shows first measurement results of three different load files with a DOD of 30%. On the left hand side is the range of DOD from SOC presented. On the right hand side are the normalized capacity fades shown. The capacity loss of the stressed cells around 75% with 30% DOD shows a proportional huge loss of capacity. However, the cycled cell around 50% SOC has just aged a little bit.

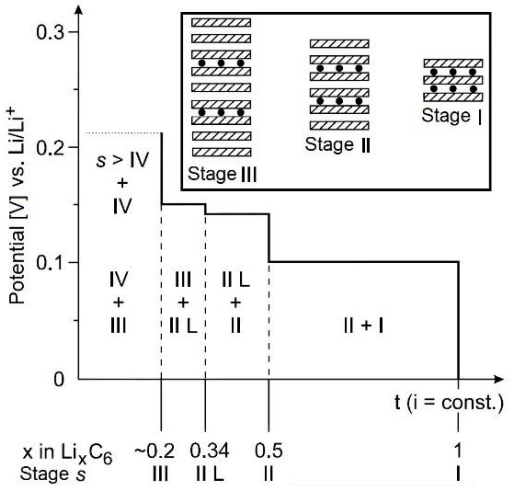

Figure 6: Stepped, electrochemical intercalation of li-ions into graphite. In addition, a schematic representation of stages 1 to 3 is shown ([6] modified according to [7]).

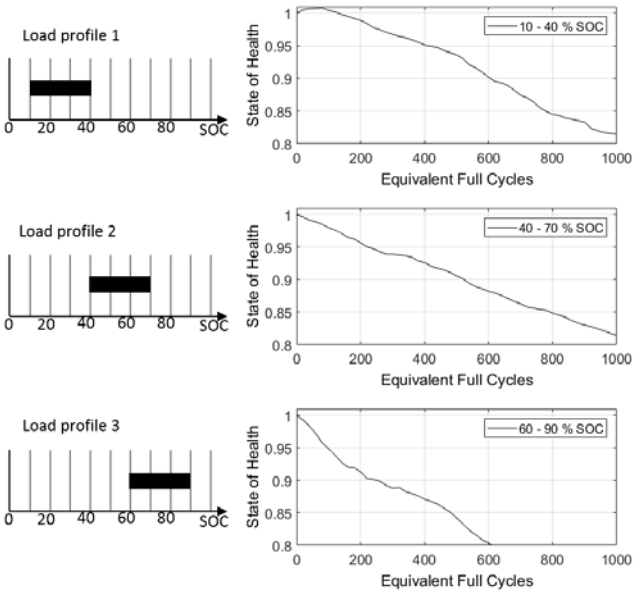

Figure 7: Load profiles of different NMC commercial cells with the aging process over equivalent full cycles at 30°C.

In order to look at the processes in more detail, separate investigations at the laboratory NMC/graphite cells were made. Presumably, aging processes can be forecasted with ongoing efforts. The following figure 8 shows a comparison of the differential voltage from a laboratory cell with the single electrodes [11]. The different peaks in figure 8, mainly at 55% SOC and at 20% SOC, are showing respective intercalation processes from lithium into the graphite anode (green). The differential capacity of the cathode is mainly a steady falling function over the

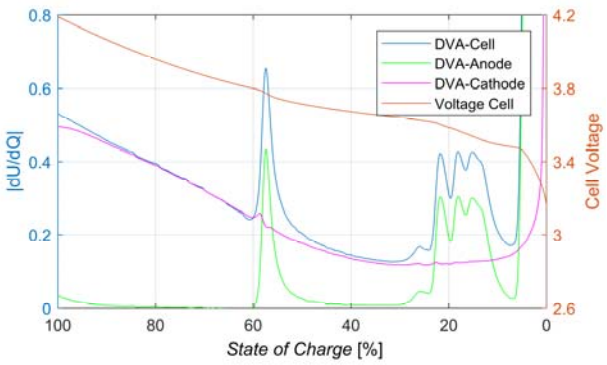

Figure 8: Comparison of the differential voltage from a complete laboratory cell: Anode vs. Li and cathode vs. Li during the charge process with C/25. Additional the charge voltage with C/25 from the cell is presented on the second y-axis.

decreasing SOC (purple).
In figure 8 is the differential voltage of a commercial cell presented. The charge rate of C/5 behaves similar to the the results of the laboratory cells and out of this circumstances it is easily transferable to the commercial cells.

Through with the laboratory cells it is possible, by considering the respective anode and cathode, to determine which of the electrodes mostly impacts the increasing aging at given loads. Further results will be presented at an advanced state of the project.

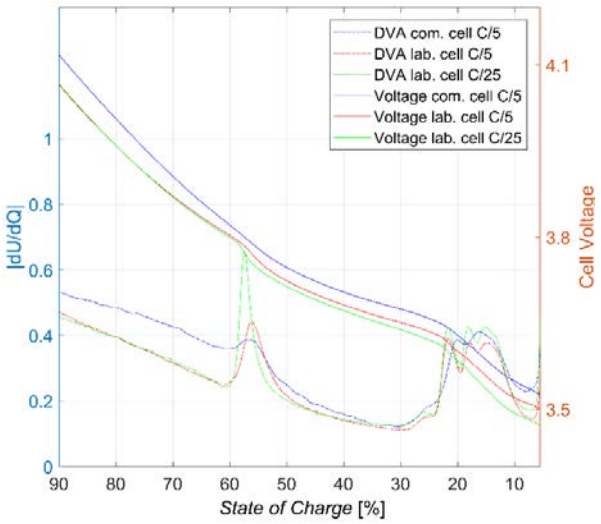

Figure 9: Comparison of the differential voltage of a laboratory cell at charge currents of C/5 and C/25 and a commercial 18650 NMC cell at charge current. Additional the cell voltages are given on the second xy-axis.

VI. DISCUSSION

The results show that the tested LFP batteries are not ideal for providing virtual inertia (cmpr. fig. 5). The first assumtion, to have an initial SOC at 50% for providing virtual inertia and adapt it to systems providing primary control power, would lead to a fast aging process. To optimize this aging behavior, the causes of increased aging at specific SOC levels were analysed. It is assumed that the intercalation stage transistion is responsible for the fast aging process. Hence, NMC/graphite cells are superior in this application field. These are often used commercially as well. Other cell types with NMC/LTO will be studied in detail in the future. First results show different aging results around 50% SOC although the anode material is equal to LFP cells. The reasons for divergent results in previous experiments have to be investigated further. Measurements with NMC/graphite have already started in the SOC range around 50% SOC with small DOD cycles.

It is also presented that there is a dependency of the loading case to the used storage system. The particular application has to be harmonized with the electrochemical storage system. By using graphite electrodes on the anode, the steps of intercalation have to be researched more precisely.

Figure 10: Chart for a superimposed controller system

For economical provision of ancillary services, like virtual inertia for grid stabilization, the battery management system (BMS) must receive and process special overlaid information of the current application.

EP2070174B1, 2007

VII. ACKNOWLEDGMENT

Supported by Federal Minitsry for Economic Affaris and Energy on the basis of a decision by the German Bundestag
Partner of the research project:

- Infineon Technologies AG
- LTI ReEnergy GmbH
- Fraunhofer Heinrich-Hertz-Institut, Faseroptische Sensorsysteme (HHI-FS)
- Stöbich technology GmbH
- AKASOL GmbH
- Assoc.: Tennet GmbH, HarzEnergie Netz GmbH

VIII. REFERENCES

[1] H.-P. Beck et all: Technische Mindesterzeugung des Kraftwerksparks bis zum Jahr 2030 in Niedersachsen und Deutschland, ISBN 978-3-7369-9626-7, Cuvillier, Goslar 2017

[2] Y. Chen, Virtuelle Synchronmaschine (VISMA) zur Erbringung von Systemdienstleistungen in verschiedenen Netzbetriebsarten, Cuvillier, 2016

[3] R. Benger, L. Beushausen, H. Wenzl, H.-P. Beck: Aging of lithium-ion batteries in high dynamic applications, Kraftwerk Batterie, 26.-27. April 2016, Münster

[4] Chen, Y.; Werther, B.; Schwake, B.; Beck, H.-P.: Netzstabilisierung durch die „Virtuelle Synchronmaschine“ (VISMA) mit überlagerter Frequenz- und Spannungsregelung, Internationaler ETG-Kongress 2013, Berlin 2013

[5] Hesse; Turschner; Beck: Die virtuelle Synchronmaschine, VDE Verlag Berlin, Etz Elektrotechnik + Automation S2/2007, pp. 38-44.

[6] Orazov; Master thesis: Identifikation und Modellbildung des Verhaltens von Lithium-Ionen-Batterien bei dynamische Belastungen, 2018

[7] Möller, K.-C.;Univ.Prof. Winter,M.: Primäre und wiederaufladbare Lithium-Batterien: Skript zum Praktikum Anorganische-Chemische Technolgie

[8] Fellberg, E. M.: Untersuchungen von Lithium-ionen-Zellen und deren Alterungseffekten: Charakterisierung und Bewertung von Materialkomponenten für Lithium-Ionen-Zellen basierend auf Benchmark- und Alterungstests mit besoineren Fokus auf die Inaktivmaterialien Binder und Seperator, 2012

[9] M. Ecker, N. Nieto, S. Käbitz, J. Schmalstieg, H. Blanke, A. Warnecke, D.U. Sauer, J. Power Sources 248 (2014) 839

[10] Kraftwerk Batterie 2016 poster presentation: Aging of lithium ion batteries in high dynamic applications

[11] EL-Cell Pat Cell datasheet: https://el-cell.com/products/test-cells/standard-test-cells/pat-cell (31.03.18) and Electrode Coins: http://www.customcells.de/elc/ (31.03.18)

[12] Petzl: Zerstörungsfreie Charakterisierung von Lithium-Plating in Lithium-Ionen-Batterien, 2015

[13] V. Sethuraman, L. Hardwick, V. Srinivasan and R. Kostecki: Surface Structural Disordering in Graphite upon Lithium Intercalation/Deintercalation, 2010

[14] H.P.-Beck et al., Konditionierungseinrichtung für Energieversorgungsnetze, Patent